Maximizing the Performance of a 3D Printed Heat Sink by Accounting for Anisotropic Thermal Conductivity During Filament Deposition

Matthew Smith[1,2], Seokpum Kim[2,3,4], Alexander Lambert[2], Maxwell Walde[3], John Lindahl[2], Kaustubh Mungale[4], Thomas Bougher[1,3], Ahmed Arabi Hassen[2], Vlastimil Kunc[2]

[1] TCPoly, Atlanta, Georgia 30309, USA
[2] Oak Ridge National Laboratory, Oak Ridge, Tennessee 37830, USA
[3] Georgia Institute of Technology, Atlanta, Georgia 30332, USA
[4] University of Tennessee Knoxville, Knoxville, Tennessee 37996 USA
Email: kuncv@ornl.gov

ABSTRACT

Newly developed high thermal conductivity polymer composite 3D printing filaments are used to characterize the thermal properties as a function of print orientation. The thermal conductivity of a printed part is anisotropic and varies by 2 – 6 times depending on the print direction – demonstrating higher conductivity in the deposition direction (in-plane) than in the two directions perpendicular to the deposition direction (cross-plane and through-plane). Therefore, deposition path planning greatly affects the overall heat dissipation rate and the performance of the heat sink. Traditionally, 3D printing slicers generate deposition paths based solely on geometric constraints. This work investigates a new approach of deposition path planning assisted by computational predictions of the heat sink thermal performance. The proposed approach uses a thermal simulation of a 3D-printed part, accounting for the anisotropic thermal properties, and the orientation of the local material properties are assigned based on the deposition path in multiple print orientations. The performances predicted via the simulations are compared, and the optimal deposition path is determined. For the highest thermal conductivity 3D printing filament (~12 W/m-K in-plane), a heat sink printed with the print direction parallel to the fins z-axis had ~20% improved performance in comparison to a heat sink with print direction perpendicular to the fins z-axis. Moreover, a plastic 3D printed heat sink was able to perform within 7% of an extruded Aluminum heat sink with similar geometry under natural convection. The computational predictions show the same trend as experimental measurements using 3D printed heat sinks.

KEY WORDS: thermally conductive filament, 3D printing, Fused Filament Fabrication (FFF), Computational Prediction, Heat sink

INTRODUCTION

As society continues to become more dependent upon electronics and increasing computational power, heat removal from electronic devices is a growing challenge. Heat removal is typically achieved through the utilization of thermal management devices including heat sinks, heat exchangers, cold plates, and heat spreaders. These devices are used to spread and conduct heat over large surface areas for convective transfer into the surrounding fluid. Metals such as Copper and Aluminum are the most commonly used materials for the fabrication of heat transfer devices because they exhibit high thermal conductivity of ~400 W/m-K and ~200 W/m-K, respectively. Although plastics offer the potential advantages of being low cost, light weight, corrosion resistant, and electrically insulating, their relatively low thermal conductivity of ~0.1-0.5 W/m-K severely limits their use in heat transfer applications.[1]

High filler loadings (>25 wt%) of thermally conductive carbon fibers, carbon black, ceramics, heat conducting nanomaterials, and other thermally conductive fillers are utilized to increase heat conduction in thermoplastic composite materials.[2-4] There are several commercial suppliers of injection molding and extrusion grade resins with thermal conductivity ranging from ~2-30 W/m-K. These materials have greater than an order of magnitude improvement in thermal conduction compared to traditional plastics and allow for the fabrication of composite parts for both metal replacement and to replace non-filled plastics. A primary application of these materials is electronics cooling including thermal management of LED lighting devices.[5]

Recently, thermally conductive thermoplastic composites have been formulated for use on low cost Fused Filament Fabrication (FFF) 3D printers.[6-8] This is an especially useful development because 3D printing allows for high surface area and complex geometries that are crucial for heat transfer, but difficult to manufacture through traditional methods. Moreover, due to filler shear induced alignment during processing, thermally conductive plastic composites have anisotropic thermal conductivity and FFF 3D printing allows for precise control of extrusion direction (toolpath) relative to a heat source. Hence, 3D printing enables engineers to create printing toolpaths where heat sink printing orientation maximizes heat removal.[7] This ability to control property anisotropy throughout results in parts that can have higher performance relative to injection molded counterparts.

This manuscript has been authored by UT-Battelle, LLC, under contract DE-AC05-00OR22725 with the US Department of Energy (DOE). The US government retains and the publisher, by accepting the article for publication, acknowledges that the US government retains a nonexclusive, paid-up, irrevocable, worldwide license to publish or reproduce the published form of this manuscript, or allow others to do so, for US government purposes. DOE will provide public access to these results of federally sponsored research in accordance with the DOE Public Access Plan (http://energy.gov/downloads/doe-public-access-plan).

This work investigates the relationship between thermal conductivity, print orientation and part performance in high thermal conductivity fused filament fabrication (FFF) 3D printed parts. The anisotropy in cross-plane, through-plane, and in-plan thermal conductivity is measured for three grades of thermally conductive composite filaments (ranging from a 10x to 50x improved thermal conductivity relative to unfilled plastic). A simple finned heat sink model is used to generate G-codes (most common numerical control programming language) with various print orientations and the orientation of local material properties are imported directly into a finite element thermal simulation powered by Abaqus. The model is used to predict heat sink thermal performance as a function of print orientation and filament thermal conductivity. The simulation results are compared to experimental thermal measurements of 3D printed heat sinks and an Aluminum heat sink with similar geometry. This work proves the importance of print orientation of 3D printed heat transfer devices and will motivate future efforts to develop slicing software that is able to generate toolpaths optimized for heat conduction.

MATERIALS AND METHODS

Thermal characterization of 3D printed heat sinks

The 1.75 mm diameter thermally conductive 3D printing filaments are provided by TCPoly, Inc. and are measured as supplied. Three compositions varying from low (3.6 W/m-K) to medium (5.7 W/m-K) to high (11.9 W/m-K) in-plane thermal conductivity are utilized for 3D printing. Samples are printed using a Flash Forge Creator Pro equipped with a Flexion extruder with a nozzle diameter of 0.8 mm, layer height of 0.5 mm, print speed of 2500 mm/min, nozzle temperature of 230°C, and bed temperature of 40°C. For each filament, the cross-plane, in-plane and through-plane thermal conductivity is measured under the prescribed print settings. Figure 1 below illustrates the definition of the in-plane, through-plane, and cross-plane thermal conductivity relative to print orientation for >20 layers of a thin, 2 line thick fin printed up from the printer bed

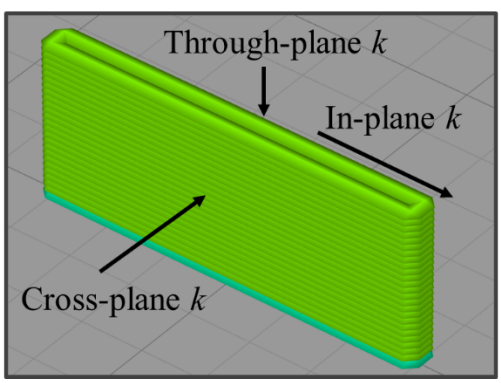

Figure 1: Printing directions and the corresponding conductivity. In-plane k is the conductivity (k_x) of the deposition direction (x). Cross-plane k is the conductivity (k_y) in the perpendicular direction (y) of x-direction on the printing layer. Through-plane k is the conductivity (k_z) in the normal direction (z) to the printing layer.

A modified 1D reference bar method is used to determine material thermal conductivity as a function of print orientation. This method follows the ASTM D5470 standard and is explained in detail in several publications.[9, 10] In short, a sample is inserted between an upper and lower reference bar where the upper bar is heated and the lower bar is cooled. Thermocouples are placed along the bar to measure the temperature profile and temperature drop from the upper heated bar, through the sample, and along the lower cooled bar. The steady state thermal profile (the temperature drops as a function of distance) is used in accordance with Fourier's Law of conduction to determine power and the sample thermal resistance (including contact resistance between the sample and the reference bars) is calculated using the heat flux, temperature profile, and sample cross-sectional area. Three thicknesses are measured for each sample and a linear regression line is used to determine and remove bar contact resistance. Finally, the sample thickness and the slope of the regression line (resistance as a function of thickness) is used to calculate thermal conductivity. The samples in this work are measured with an upper bar temperature set to 100°C and lower bar maintained at 15°C. The samples cross-sectional area is 1 cm x 1 cm and the clamping pressure is 75 N/cm^2.

Generic heat sinks with a base area of 100x100 mm (2 mm base thickness) and a total of 10 evenly spaced 40 mm tall fins with 1.6-2 mm thickness were printed in two distinct orientations. The first orientation, referred to as "horizontal" throughout, results in a heat sink with the in-plane thermal conduction path oriented perpendicular to the heat sink base as illustrated in Figure 2 below. Both the heat sink fins and the 2 mm thick base are printed with the through-plane orientation relative to the heat sink base.

Case 1: Horizontal Printing

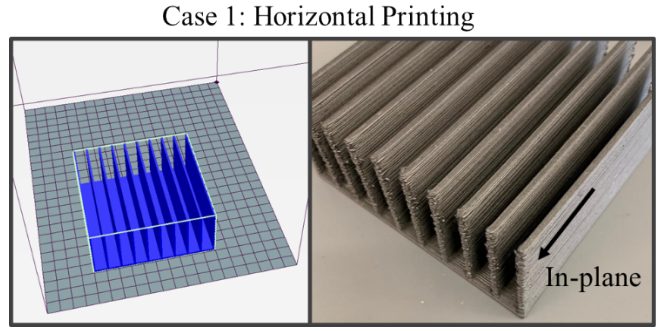

Figure 2: Printing heat sink in horizontal direction. The in-plane printing direction is perpendicular to the direction of heat conduction from the heat sink base to the fin edge.

Figure 3 represents the second orientation investigated where the heat sink is printed up "vertically" from the print bed with the in-plane thermal conduction path oriented parallel to the heat sink base in the heat sink fins. In this orientation, the 2 mm thick heat sink base is printed in an orientation where the cross-plane thermal conductivity is oriented parallel to the base surface. Hence, heat will transfer through the base in the cross-plane orientation and then into the fins in the in-plane orientation. No post processing was completed on the heat sinks and the surfaces are generally rough and slightly structured as an artifact of the 3D printing layer by layer deposition process.

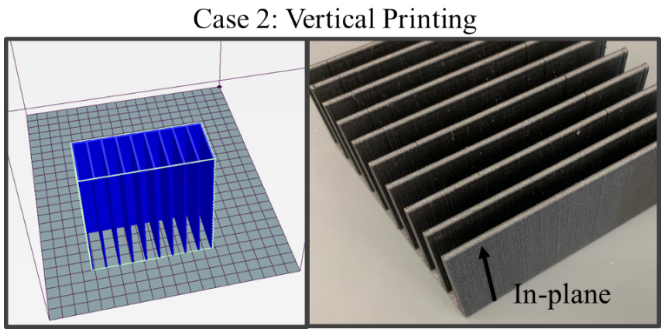

Figure 3: Printing heat sink in vertical direction. The in-plane printing direction is parallel to the direction of heat conduction from the heat sink base to the fin edge.

A 45-Watt insulated heating pad in thermal connection to each heat sink is used to simulate a heat source and to determine each heat sinks ability to efficiently dissipate heat. Figure 4 is included to demonstrate experimental set-up for heat sink performance characterization. A 45W square heating film with adhesive is pressed on a 100x100 mm (2 mm thick) aluminum plate. Thermal tape of 500 micron thickness and through plane thermal conductivity of 2 W/m-K is placed on top of the aluminum plate. A fine gauge thermocouple is placed on top of the thermal tape with the temperature measurement point located directly in the center of the 100x100 mm thermal tape square. A <1 mm wide slit was cut in the thermal tape to make a channel for the thermal couple wire to sink between the heat sink and aluminum plate. Each heat sink is centered on and placed in contact with the thermal tape and the steady state temperature of the thermal couple is recorded. Ambient temperature is 25°C for all measurements and heat loss at the heater is minimized through insulation of the heating pad. An Aluminum extruded heat sink with identical fin count and geometry was used to compare to the 3D printed heat sinks. It is worth noting that the Aluminum heat sink weighs ~2x the plastic heat sinks due to increased material density.

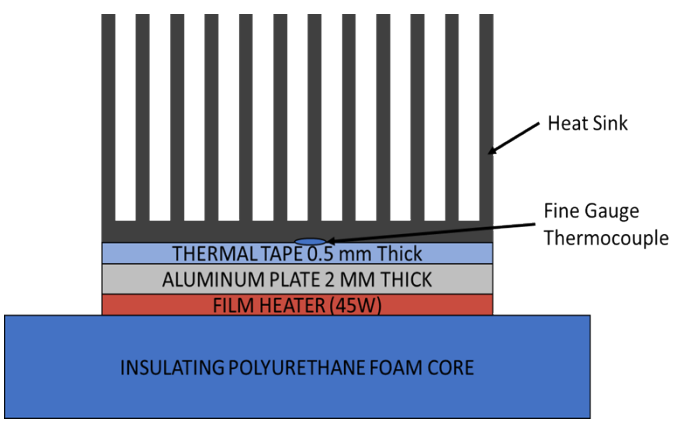

Figure 4: Experimental set-up for heat sink performance characterization

Performance Simulation

The operational temperature of a heat sink with identical geometry to the printed samples is analyzed via computational simulation. Figure 5 shows the design and the dimensions of the heat sink with the operational conditions. The bottom surface is attached to a heat source with the heat rate of 45 W and he heat sink is installed in the open air under natural convection.

For the simulation, the heat source is assumed to be evenly supplied to the entire bottom surface of the heat sink and the air temperature is set to 25 °C. The simulation utilizes Finite Element Method (FEM) with 4k hexahedron elements and a quadratic interpolation function. The simulation accounts for conduction, convection, and radiation. The simulation does not explicitly model the air flow near the heat sink or the fluid-structure interaction. The constitutive relation of convection used in the simulation is the Newton's law of cooling with a constant heat transfer coefficient (h). Thermal radiation is governed by the Stefan-Boltzmann law with a constant emissivity (ε). Convection and radiation are applied to the entire surfaces of the heat sink except the bottom surface. Conduction is governed by the three-dimensional Fourier's conduction equation with three conductivity parameters (k_x, k_y, k_z) for x, y, and z directions, respectively. The directions of x, y, and z are not from the geometric global coordinate system. Instead, the directions are from the printing directions. The direction of x is the deposition direction (= printing nozzle movement direction), y-direction is the perpendicular direction of x-direction on the same plane (= printing layer plane), and z-direction is the through-plane direction (= normal to the printing layer). Therefore, once the build orientation is determined, z-direction is fixed. The directions of x and y change as the nozzle movement changes.

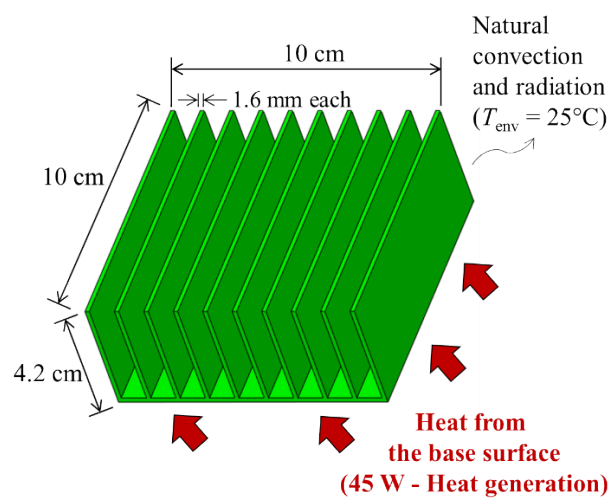

Figure 5: Heat sink design and the dimensions. A uniform heat rate of 45W is supplied to the base surface of the heat sink. The other surfaces are exposed to the air (T_{env} = 25°C)

Compton et al. [11] used the convection coefficient of h = 8.5 W/(m^2□K) and the emissivity of ε = 0.87 for a 3D-printed wall with a reinforced polymer. Based on similarities in composition, an emissivity of ε = 0.87 is used in this work for the 3D printed heat sinks with polymers. The wall is 1.5-meter long in their model and it is a single wall, whereas our heat sink is 0.1-meter long and it has multiple fins. The convection coefficient is known to be highly dependent on size, shape, and the gap between walls (or fins), whereas the emissivity is highly

dependent on the material. For a heat sink with relatively similar size and shape to our model, Lee et al. [12] reported h = 5.5 – 8 W□(m²□K) and Yu et al. [13] reported h = 4 – 6.5 W/(m²□K). We chose the convection coefficient of h = 6 W/(m²□K) for polymers and aluminum. For aluminum, we used the emissivity of $\varepsilon = 0.1$ as measured in Ref. [14].

Because the directions of x and y are not uniform for a given geometry and a given build orientation, the orientation vector must be assigned in each element in Finite Element (FE) mesh. Figure 6 shows the technique implemented in the simulation. The simulation consists of two-stage process. At the first stage, the elements are activated along the toolpath described in Gcode for 3D printing. During the activation process, the orientation vector is assigned in each element. The orientation vector is parallel to the toolpath direction determined by Gcode. Once the element activation process is done, the data of the orientation vector of all elements are transferred to the heat transfer simulation model at the second stage.

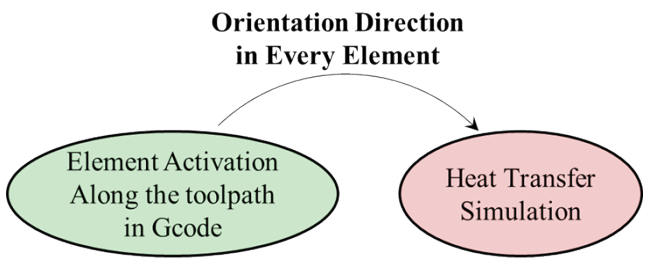

Figure 6: Two-stage process for the heat sink performance simulation. At Stage 1, elements are activated along the toolpath and the orientation vectors are assigned in the elements. At Stage 2, the data of the orientation vectors are transferred, and heat transfer simulation is performed.

Figure 7 shows the element activation process of the two cases – Case 1 for the horizontal printing and Case 2 for the vertical printing. The toolpath in Gcode is imported and the elements located along the toolpath are activated. During the activation process, the orientation vector is determined as the parallel direction to the toolpath direction. The blue arrow in Fig. 7 shows the element orientation vectors.

RESULTS AND DISCUSSION

Material thermal conductivity (***k***) as a function of print orientation is included in Table 1. In general, the in-plane k is three to six times of the through-plane k, and the anisotropy increases as the thermal conductivity increases. The cross-plane k is approximately two times of the through-plane k and is not significantly different between the three measured samples. The through-plane thermal conductivity increases slightly from the low k to medium k material and then plateaus. All conductive polymers used in this study have 10 to 100 times higher conductivity than PLA (k = 0.13 W/m·K).

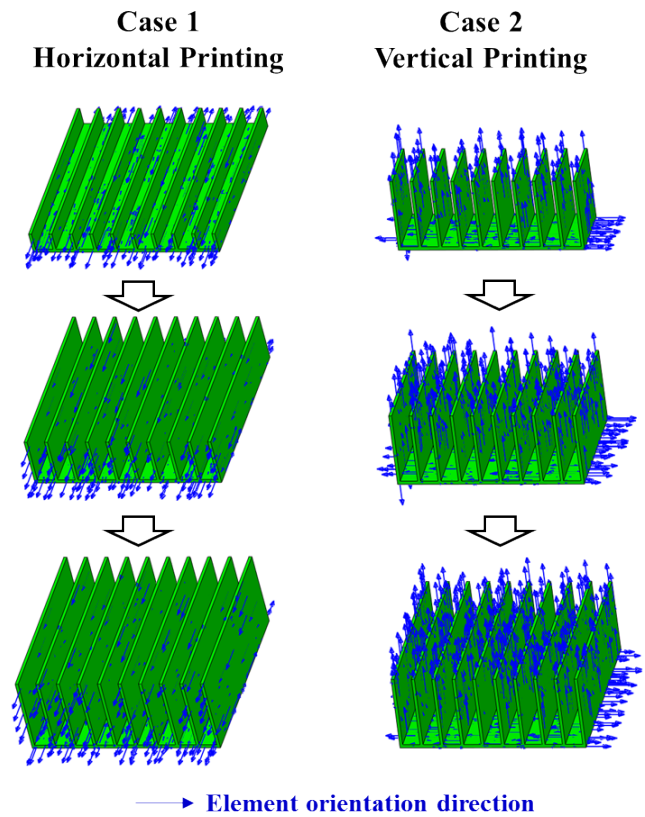

Figure 7: Element activation along the toolpath in Gcode for (a) Case 1 – Horizontal printing and (b) Case 2 – Vertical Printing

The cross-plane and through-plane thermal conductivity are limited due to alignment of the thermally conductive filler materials during extrusion and due to interfaces between print lines. For example, at a layer height of 0.5 mm, a 2 mm think material will have 3 interfaces in which heat must transfer through for the through-plane measurement. On the other hand, a 2 mm thick sample with 0.8 mm line thickness will only have 2 interfaces heat must transfer for the cross-plan direction. It is expected that these values may change significantly as a function of layer height and nozzle diameter and future studies have been initiated to explore further.

Table 1: Thermal conductivity of the three types of filament

Material	Filament Thermal Conductivity k [W/(m□K)]		
	Through-plane (k_3)	Cross-plane (k_2)	In-plane (k_1)
Low k	1.6	3.4	3.6
Mid k	2.1	3.5	5.7
High k	2.0	4.3	11.9

To understand the effect of conduction, a simple analytical one-dimensional approach is used to estimate the surface temperature. Figure 8 shows a schematic diagram. The heat flux of $\dot{q} = 563^{\mathrm{W}}/\mathrm{m}^2$, based on the heat supply of 45 W and the fin area of 800 cm², is applied. The length of the conductivity resistance is 20 cm (half of fin height), and the environment

temperature (T_{env}) is 25 °C. The convection coefficient of $h = 6$ W/(m^2□K) is used (natural convection approximation).

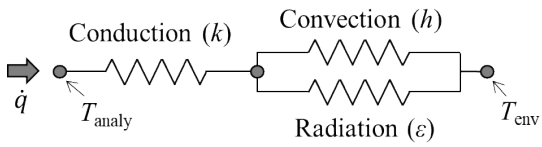

Figure 8: Schematic diagram of a simplified one-dimensional heat transfer model. This model is used for an analytical solution, not for a numerical simulation.

Figure 9 shows the temperature as a function of conductivity with two different emissivities (ε = 0.1, 0.87) for the simple one-dimensional model under natural conduction. The solid line indicates the temperature curve for high emissivity, and the dotted line indicates the temperature curve for low emissivity. The difference of the temperature between low and high emissivity is nearly 40 °C. However, this is a simplified case where emissivity is more significant than what would be observed in a finned heat sink where the fins primarily radiate heat between each other. Moreover, radiational heat loss has often been excluded for heat sink performance prediction and neglecting radiation (i.e., $\varepsilon = 0$) is acceptable if the heat sink material has very low emissivity or if the geometry results little heat loss from radiation (such as this case). However, as studied in Ref. [15], radiation can be a significant source of heat loss if the emissivity is not a negligible value. For both cases (low and high emissivities), if conductivity is small ($k < 1$), temperature is highly affected by the change in conductivity. With high conductivity ($k > 10$), further increasing conductivity has a minimal impact on temperature and total thermal resistance is dominated by convection as opposed to material thermal conductivity. The performance is more sensitive to material thermal conductivity below 2 W/m-K, hence, these moderately conductive materials have performance most comparable to aluminum when under natural convection and with thermal conductivity >2W/m-K..

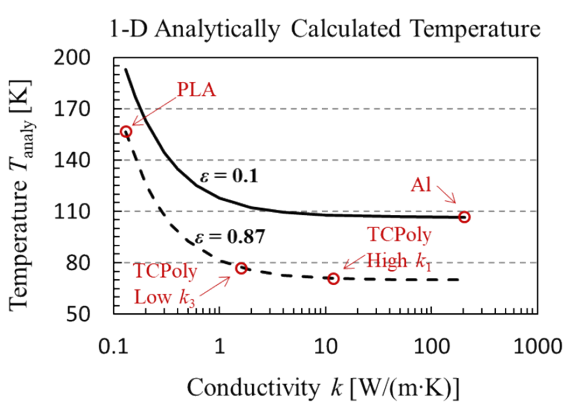

Figure 9: Analytically calculated temperature from one-dimensional model in Fig. 8.

Simulation is performed with the original geometry as in Fig. 5. The orientation vectors assigned as shown in Fig. 7 and the thermal conductivity measurements from Table 1 are transferred to the heat transfer simulation. Therefore, the heat transfer simulation is able to account for an accurate representation of the effect of printing direction. Moreover, because the conductivity in the in-plane direction (= deposition direction) is much higher than the conductivity in the through-plane direction (= normal direction to the printing layer plane), the cooling performance of Case 2 is higher than that of Case 1, as shown in Fig. 10 (simulation results for the high thermal conductivity filament print in each orientation). The colormap represents the temperature predicted via simulation where red indicates high temperature and blue indicates low temperature. The base temperature of Case 1 is higher than that of Case 2 by approximately 50°C for the high thermal conductivity filament.

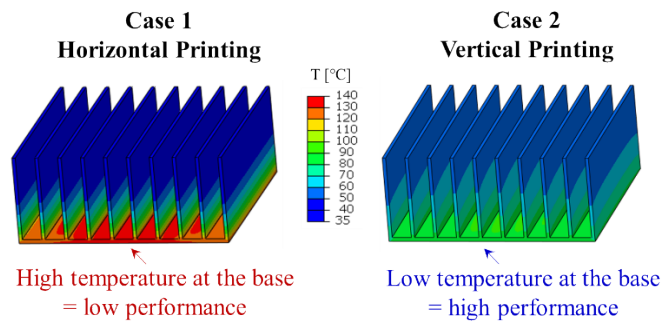

Figure 10: Temperature profile of Case 1 and Case 2 predicted from heat transfer simulation accounting for the effect of printing direction.

The maximum temperature of the heat sink printed in both orientations and at each thermal conductivity value is predicted from simulation and is also measured from experiment. Experimental details for the heat sink thermal measurements are provided in the Materials and Methods section. The results from the experiment and the simulation are summarized in Table 2 and illustrated in Figure 11. Unfilled PLA and aluminum heat sinks with similar geometry are included for comparison.

Table 2: Maximum temperature of heat sink from simulation and experiment with various materials.

Material		Experiment Max T [°C]	Simulation Max T [°C]
PLA		N/A	267*
Case 1 Horizontal Printing	TCPoly-Low k	134	155
	TCPoly-Mid k	135	144
	TCPoly-High k	134	145
Case 2 Vertical Printing	TCPoly-Low k	123	127
	TCPoly-Mid k	117	112
	TCPoly-High k	113	94
Aluminum		107	99

* The simulation does not account for the phase change at the melting temperature

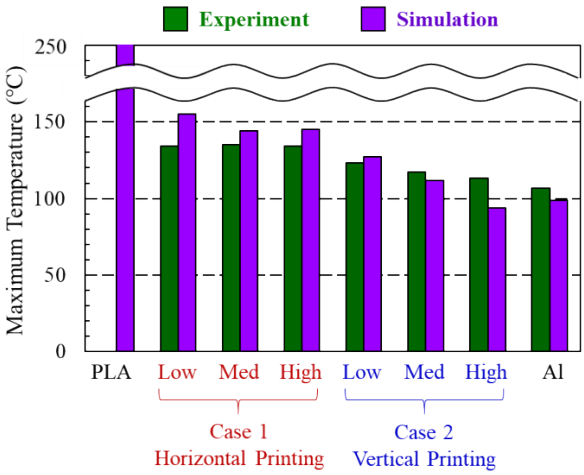

Figure 11: Visual representation of Table 2. Maximum temperature of Case 2 is in general lower than that of Case 1. The maximum temperature of high conductivity polymer in Case 2 is close to that of aluminum.

The simulation shows that the maximum temperature of the PLA heat sink would be ~100°C higher than the worst performing low thermal conductivity TCPoly heat sink. The simulation does not account for the phase change of PLA at its melting temperature and the PLA heat sink was not experimentally tested due to material melting and warping. Overall, the maximum temperature from Case 1 is consistently higher than that from Case 2. Moreover, for the high thermal conductivity filament, there is ~20% improvement in heat sink performance when the heat sink is printed in the vertical direction. The high thermal conductivity heat sink printed in vertical direction shows slightly higher temperature than the heat sink made of aluminum, and the difference is only ~ 6 °C (within 7% performance). This similar performance despite a factor of 20 lower thermal conductivity for the plastic can be attributed to fact that under natural conduction heat removal is convection limited and conduction plays a less significant role. These results indicate that print orientation can play a significant role in heat sink thermal performance and the plastic heat sinks can exhibit similar performance to Al heat sinks under natural convection.

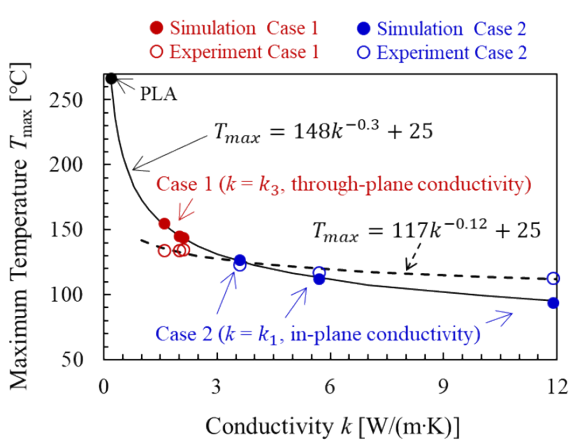

Figure 12: Maximum temperature as a function of conductivity of various polymers from simulation. The conductivity k is for the direction perpendicular to the base surface.

Simulation results show that aluminum heat sink temperature is even higher than the high k heat sink in Case 2 due to the emissivity difference, which can be heavily dependent on the Aluminum heat sink surface properties and manufacturing method. The maximum temperature can be analyzed as a function of conductivity as shown in Fig. 12. Black indicates PLA (simulation), Red indicates Case 1, Blue indicates Case 2. As the polymer conductivity increases, the maximum temperature decreases. The relationship is represented by the power law equation displayed on Fig. 12 where T_{max} is the maximum temperature. For Case 1, k values are from k_3., and for Case 2, k values are from k_1.

The difference of maximum temperature between experiment and simulation can be attributed to the following factors. (1) The heat transfer coefficients (h and ε) are not obtained from experimental measurements for the specific settings of our study, but they are from literatures with similar settings. It is possible that the Al heat sink has higher emissivity than used in the simulation here due to anodization and/or surface oxidation. (2) Printing direction determines the orientation of the surface waviness which may affect the convection coefficient (h), whereas a fixed h value is used for all simulations. (3) Conductivities of the polymers are assumed to be constant over a range of temperature. However, in general, conductivity of polymer increases with increasing temperature [16, 17]. (4) The change in polymer could result in the change of the extrusion rate, hence the changes in bead width. Therefore, the fin thickness might vary depending on the extruded polymer. The simulation, however, assumes the same fin thickness. (5) The convection coefficient (h) and the emissivity (ε) are assumed to be the same for all polymers, although these values might change depending on the printing quality of different polymers and the compositions of the polymers. (6) The heat supplied to the heat sink from the generator is assumed to be the same (45 W) for all simulations, whereas in experiment, there is an energy loss, and the amount of loss at the interface could be different as material changes. After all, the simulation results are from ideal settings.

SUMMARY

High thermal conductivity 3D printing filaments are used to determine the thermal conductivity of 3D printed parts as a function of print orientation. Filament in-plane, through-plane, and cross-plane thermal conductivity is measured, and these values are used to predict a 3D printed heat sink's thermal performance as a function of print orientation using finite element methods. Finally, the thermal performance of the 3D printed heat sinks is evaluated to determine heat sink effectiveness and model robustness. The results demonstrate an in-plane thermal conductivity ranging from 3.6 to 11.9 W/m-K and a 3-6x anisotropy ratio between in-plane and through-plane thermal conductivity. The cross-plane thermal conductivity is typically 2x the through-plane thermal conductivity. The finite element modeling shows the same trend as experimental measurements on 3D printed heat sinks. A 3D-printed

composite heat sink with in-plane thermal conductivity oriented parallel to the heat sink base (aligned parallel to the heat transfer direction) demonstrated ~20% improvement in performance relative to a heat sink printed with the same material but with the print direction oriented with the in-plane direction perpendicular to the base. Moreover, because heat removal was convection limited, a 3D printed plastic composite heat sink was able to perform within 7% of a metal at half the weight. This work will result in future efforts to enhance 3D printed part performance through toolpath optimization.

Acknowledgments

This research is sponsored by the U.S. Department of Energy, Office of Energy Efficiency and Renewable Energy, Industrial Technologies Program, under contract DE-AC05-00OR22725 with UT-Battelle, LLC.

References

1. Anderson, D.R., *Thermal Conductivity of Polymers.* Chemical Reviews, 1966. **66**(6): p. 677-690.
2. Ha, S.M., et al., *Thermal conductivity of graphite filled liquid crystal polymer composites and theoretical predictions.* Composites Science and Technology, 2013. **88**: p. 113-119.
3. Zhou, W., et al., *Thermal conductivity of boron nitride reinforced polyethylene composites.* Materials Research Bulletin, 2007. **42**(10): p. 1863-1873.
4. Chen, H., et al., *Thermal conductivity of polymer-based composites: Fundamentals and applications.* Progress in Polymer Science, 2016. **59**: p. 41-85.
5. Cho, E.-C., et al., *Graphene-based thermoplastic composites and their application for LED thermal management.* Carbon, 2016. **102**: p. 66-73.
6. Shemelya, C., et al., *Anisotropy of thermal conductivity in 3D printed polymer matrix composites for space based cube satellites.* Additive Manufacturing, 2017. **16**: p. 186-196.
7. Jia, Y., et al., *High through-plane thermal conductivity of polymer based product with vertical alignment of graphite flakes achieved via 3D printing.* Composites Science and Technology, 2017. **145**: p. 55-61.
8. Quill, T.J., et al., *Thermal and mechanical properties of 3D printed boron nitride – ABS composites.* Applied Composite Materials, 2018. **25**(5): p. 1205-1217.
9. Thompson, D.R., S.R. Rao, and B.A. Cola, *A stepped-bar apparatus for thermal resistance measurements.* Journal of Electronic Packaging, 2013. **135**(4): p. 041002.
10. Smith, M.K., et al. *Thermal Interface Material Enablement of Off-Board Two-Phase Cooling*. in *2018 17th IEEE Intersociety Conference on Thermal and Thermomechanical Phenomena in Electronic Systems (ITherm)*. 2018.
11. Compton, B.G., et al., *Thermal analysis of additive manufacturing of large-scale thermoplastic polymer composites.* Additive Manufacturing, 2017. **17**: p. 77-86.
12. Lee, J.B., H.J. Kim, and D.-K. Kim, *Experimental Study of Natural Convection Cooling of Vertical Cylinders with Inclined Plate Fins.* 2016. **9**(6): p. 391.
13. Yu, S.-H., K.-S. Lee, and S.-J. Yook, *Natural convection around a radial heat sink.* International Journal of Heat and Mass Transfer, 2010. **53**(13): p. 2935-2938.
14. Yu, S.-H., K.-S. Lee, and S.-J. Yook, *Optimum design of a radial heat sink under natural convection.* International Journal of Heat and Mass Transfer, 2011. **54**(11): p. 2499-2505.
15. Khor, Y.K., Y.M. Hung, and B.K. Lim, *On the role of radiation view factor in thermal performance of straight-fin heat sinks.* International Communications in Heat and Mass Transfer, 2010. **37**(8): p. 1087-1095.
16. Dashora, P. and G. Gupta, *On the temperature dependence of the thermal conductivity of linear amorphous polymers.* Polymer, 1996. **37**(2): p. 231-234.
17. Choy, C.L., *Thermal conductivity of polymers.* Polymer, 1977. **18**(10): p. 984-1004.